Alfarama Journal of Basic & Applied Sciences

https://ajbas.journals.ekb.eg
ajbas@sci.psu.edu.eg

Faculty of Science Port Said University

http://sci.psu.edu.eg/en/

April 2023, Volume 4 , Issue II

DOI:**https://doi.org/10.21608/ajbas.2022.157509.1119**

ISSN 2682-275X

Submitted: 2/09/2022
Accepted: 14/11/2022

Pages: 320 - 339

Characterization of the feldspar placer deposits of Umm Shaddad Area, Eastern Desert, Egypt.

Hoda R. Saad[1,*], Abu El-Hagag N. Ahmed[2] , Mona A. El-Harairey[1]

[1]Geology Department, Faculty of Science, Damietta University, New Damietta 34517, Egypt.

[2]Egyptian Environmental Affairs Agency, Red Sea Branch, Hurghada, Egypt.

***Corresponding author: hodaragab@du.edu.eg**

ABSTRACT

In the present study, placer feldspar resources in the Umm Shaddad region, Qusier, Egypt were invested to the appropriateness as raw materials for the glass and ceramic industries. Umm Shaddad area located west of Umm Gheig Lead Zinc Mine, at latitude 25°37' and 25°41' and longitude 34°19' and 34°24'. Chemical analyses revealed that the SiO_2 content in the analyzed feldspar placer deposit, is an average of 74.16%. This value is higher than that required for glass industries but lower than the commercial average of ceramic industries. When compared to the commercial average for glass and ceramic sectors, the average content of Fe_2O_3 (2.48%) is considered high. The average K_2O content in the analyzed samples is 4.77%, which is higher than the commercial values. Na_2O content averages 3.05% and Al_2O_3 averages 11.79%, which are lower than the commercial average for the glass and ceramic sectors. The radiometric effect of the raw feldspar of Umm Shaddad was also evaluated. Activity index of Gamma (I_γ) and Alpha (I_α), Radium equivalent activity (Ra_{eq}) and Hazard indices (H_{ex} and H_{in}) are lower than the acceptable world value. However, the total Annual effective dose equivalent (AEDE) of the studied samples ranged between 0.82 to 1.261 with an average 1.137 which is higher than that of the world's acceptable values. In conclusion, although the feldspar placers of Umm Shaddad have suitable content of oxides after minor treatment while, the high values of total Annual effective dose equivalent (AEDE) diminished its use for either ceramic or glass industries.

Key Words:

Feldspar, Oxides, Radioactive, Umm Shaddad, Egypt.

1. INTRODUCTION

Granitoides are the major source of fluxes, after albitites, having fulfilled about 19% of the overall ceramic demand in the period 1970-2015 [1]. Alkali feldspars are the primary raw minerals used in the ceramic and glass industries. More than 70 nations have feldspar economic reserves, and more than 50 countries currently supply the majority of the world's feldspar production, which in 2006, 20 Mt of feldspar, 1.4 Mt of nepheline syenite, and 1.4 Mt of aplite, phonolite, and China stone [2]. Egypt was one of many nations with feldspar reserves. In 2022, some 400,000 metric tons of feldspar were produced in mines all over Egypt, [3].

Over 90% of all material produced is used in the ceramics and glass industries, which also use feldspar minerals. The production of glass products uses more than 70% of feldspar, while ceramics and other items use 30%. Izquierdo Pazo et al., [4] shown that the low rate and balanced melting of feldspar across the necessary temperature range makes it stand out. Owing to its assistance in the melting of clays and quartz, this is of almost significance for the production of both glass and ceramics. In terms of its chemical and physical qualities, feldspar must meet particular grade and specification requirements for use in the ceramic and glass industries [5]. Sinai [6–8] and the Eastern Desert [9–10] worked on the granite. The overall output from Ras Mohamed, Sinai, Egypt over the period 1970-2015 was estimated by 3 million tons [1]. The potential of yet unexploited granitoid sources appears to be outstanding in some areas, like the Egyptian Eastern Desert [11; 12, 13].

The present study characterizes the mineral composition and radiometric impact of the feldspar placer deposits of Umm Shaddad area, Eastern Desert, Egypt, to study their applicability to use in glass and ceramic industries.

2. Geology & Geological setting

Umm Shaddad area located west of Umm Gheig Lead Zinc Mine, at latitude 25^{o}37' and 25^{o}41' and longitude 34^{o}19' and 34^{o}24' **(Fig. 1)**. It could be reached from umm Gheig through the desert road running to the west of Wadi Umm Gheig for about 20 Kilometer. General outline topography shows that the area is built up of a series of separated granitic masses in which the largest of them is Gabal Umm Shaddad of around 770m above the sea level. These basement rocks exposed in the area of study are mainly arranged starting from the oldest as metavolcanics, metagabbros, granpdiorites, younger gabbros, monzogrznites, syenogranites, alkaline granites and alkaline syenites. A geological map at scale 1:50000 for the study area were modified after [14] **(Fig. 2).** Granitoids associated to volcanic rocks with a basaltic composition can be found in the rocks of the Umm Shaddad district. [15]. Sabet [16] discussed that the granitic intrusion of Umm Shaddad is oval shaped and tectonized xenolitic granitic masses, fine to coarse grain size usually porphyritic composed essentially of alkaline feldspars and quartz and minor amounts of chlorite, sphene, apatite, epidote, zircon and little iron oxides. Umm Shaddad granitic masses are a discordant with the enclosing metamorphic rocks, where the boundary is substantially concordant with the foliation of the metamorphic rocks, **(Fig. 2** and **Fig. 3)**. The red granites are sometimes crushed and tectonized to varies extents. Wadi Um Lassifa is the main wadi draining the high granitic hill ranges and peaks of G. Um Shaddad. This wadi has a general NE-SW trend. The granitic weathering products are concentrated in two tributaries wadies. These are Khore Umm Shaddad and Kab Ahmed. The main wadies and tributaries are covered by weathering products of granitic from the country rocks on their sides or upstream. Khore Um Shaddad runs in the west- east direction for about 2km.of average width of this Khore about 250m. The alluvium filling depth ranges from 1-4 m of elevation 294-273 m.

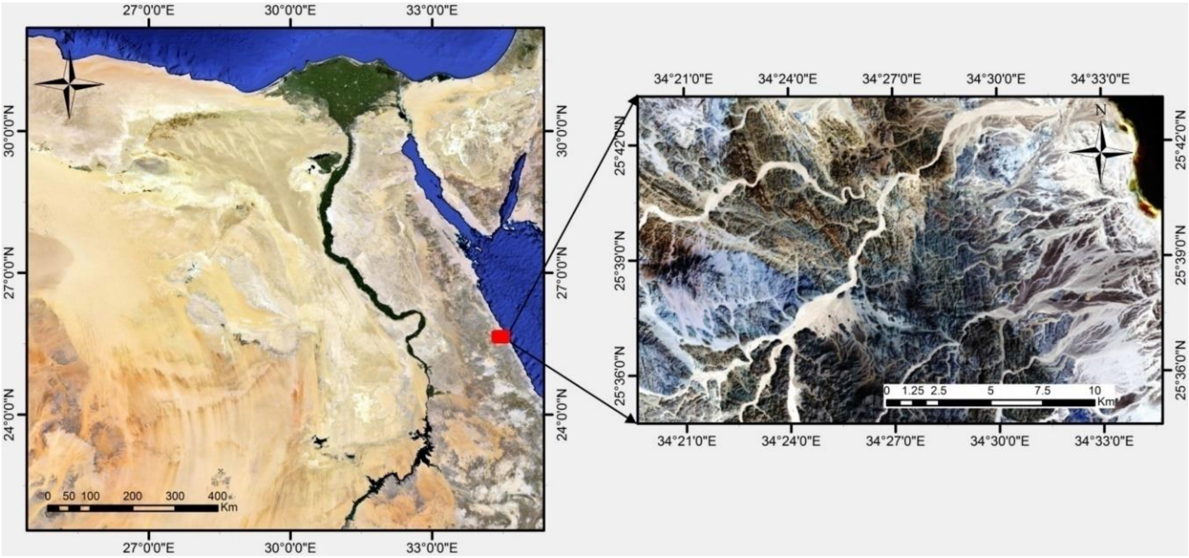

Figure 1. Location map of Umm Shaddad area, Egypt.

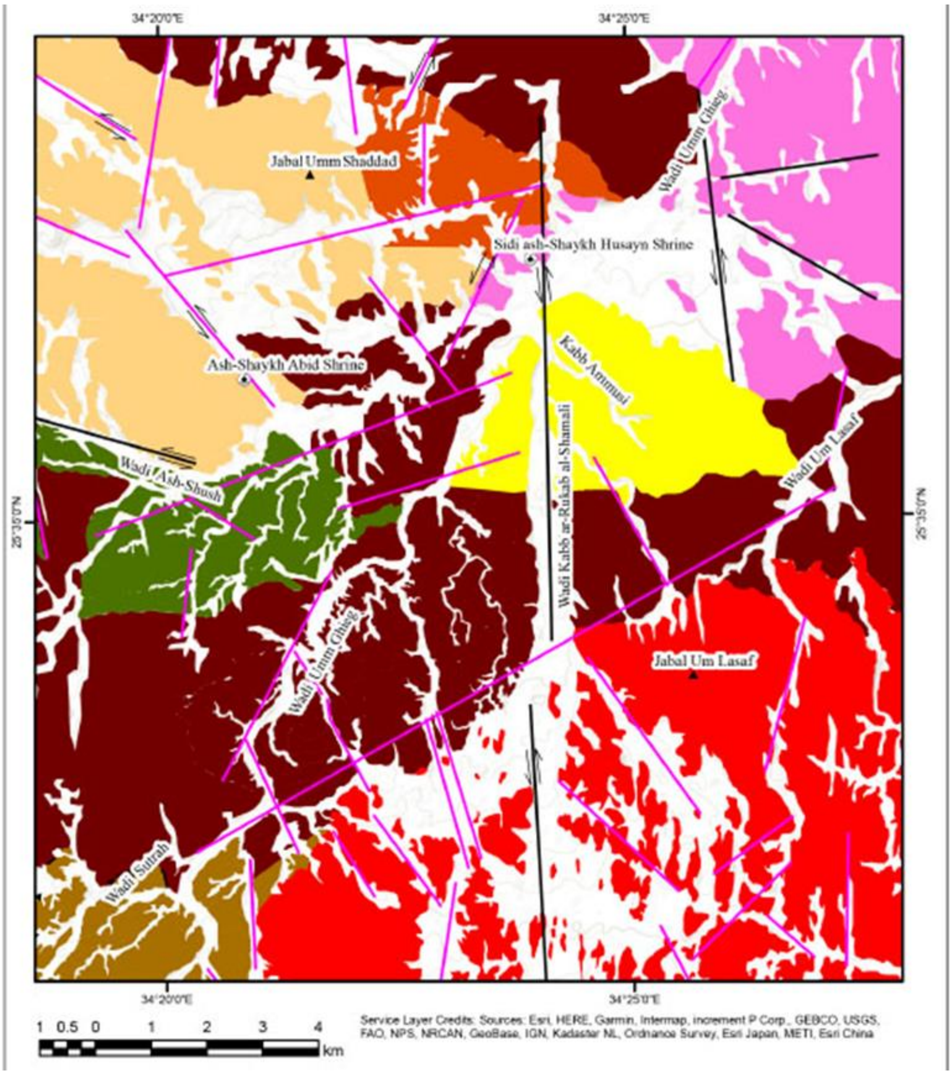

Figure 2. Geological map of Umm Shaddad area, Egypt modified after Conoco Coral (1987).

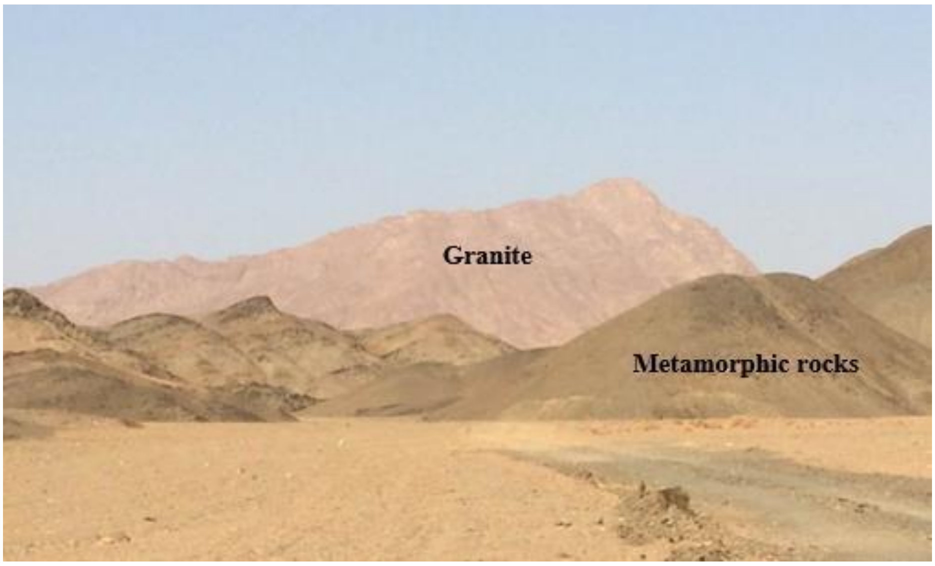

Figure 3. Photograph showing Umm Shaddad granite and the surrounding metamorphic rocks.

3. Methodology

Thirty-five samples were collected from four vertical sections to cover the studied placer deposit body. The distance between the sections are about 100 meters; section one and two form the largest alluvial fans at the Northern side of Umm Shaddad granitic body, section three from small fan at the same side. These three sections represent Khore Umm Shaddad alluvium sediments. While, section four collected from the fan at the South side of Umm Shaddad granitic body. The samples from each vertical section were taken from the base to the top every 25 cm. Section number one yielded ten samples., 6 samples from section no. two, 4 samples from section no. three and 15 samples from section no. four **(Fig. 4a)**. All the placer deposits showing several cycles of sedimentation and finning upward, **(Fig. 4b).** All of the samples underwent mechanical analysis fractionate the sediments into 7 grain sizes and size was investigated by binuclear microscope to identify the mineralogical composition and the relative abundance of minerals to each other. The mineralogical composition was determined using X-ray diffractometer (PW3710, in the Egyptian Nuclear Material Authority). Chemical analysis was done on seven selected samples (placer feldspar) to measure the major oxides which were done in Acme Labs (Toronto, Canada) by using ICP- MS method (is the analytical technique that uses an Inductively Coupled Plasma to ionize the sample, which provides a lower detection limit down to ppt). Twenty-three samples were chosen to represent the four vertical sections at Umm Shaddad area to evaluate the radiometric effect. After being filled and tightly sealed, cylindrical cans made of plastic with a 212 cm2 volume, 9.5 cm diameter, and 3 cm height were left for more than 30 days to gather free radon and reach radioactive equilibrium before being counted with a -ray spectrometer and then subjected to laboratory tests at the Egyptian Nuclear Material Authority to determine the content of (U, Th, Ra and K) as eU, eTh, Ra, and K%.

A. **B.**


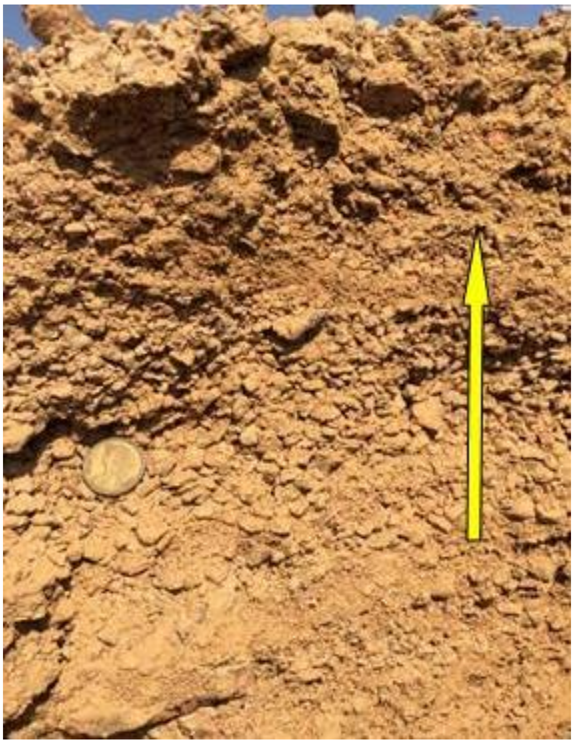

Figure 4. A. Photograph showing the sampling (white arrows). B. Photograph showing cyclisty and finning upward of placer deposits (yellow arrow) at Umm Shadad area, Egypt.

4. Results and Discussion

4.1. Mineralogical composition

4.1.1. A-Mechanical analysis and mineralogical identification:

A representative amount of minerals in sand size (nearly about 0.1 gm, about 700-1000 grains) took by quartering from each sample and sprinkled on a glass slide, to be fixed under the was investigated under the binuclear stereomicroscope, and the weight percent of each mineral in the different samples was calculated. This method reveal that the studied samples composed of quartz, feldspars, ferromagnesian minerals (mica) and opaque minerals. The percentage of minerals composition different from sample to another. In which the feldspars comprise the essential mineral which range from 56.5% to 88.6% followed by quartz, which constitute the range of composition from 8.1% to 31.32% and the ferromagnesian and opaque minerals ranged in composition from1.17% to 19.6%.

4.1.2.B- X-Ray Diffraction analysis

The composition of the minerals was established using X-ray diffractometer (PW3710) for four samples. Each sample is a representative for each vertical section. These analyses revealed that the mineralogical compositions are anorthoclase, quartz, phlogopite, hematite, kaolinite (**Fig. 5**) and are listed in **Table 1**.

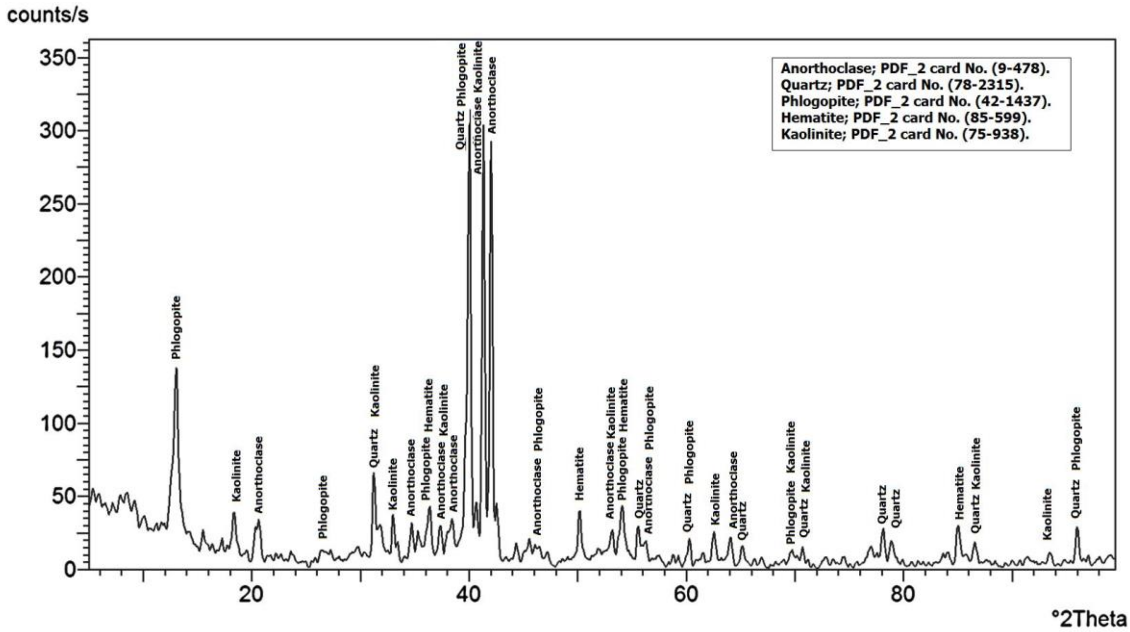

Figure 5. The mineralogical composition of a selected sample determined using X-ray diffractometer (PW3710).

Table 1. X-Ray Diffraction analysis for the selected samples.

Ref. Code	Compound Name	Chemical Formula
9-0478	Anorthoclase	(Na, K) (Si_3Al) O_8
78-2315	Quartz	SiO_2
42-1437	Phlogopite	K (Mg, Fe)$_3$ (Al, Fe) Si_3 O_{10} (OH, F)$_2$
85-0599	Hematite	Fe_2O_3
75-0938	Kaolinite	$Al_2Si_2O_5$ (OH)$_4$

4.1.3.C- Chemical composition of Um Shaddad feldspar

Estimation of feldspar deposits at Wadi Umm Shaddad was performed using 35 samples from the four trenches. Chemical analyses were done to selected 7 samples of the raw feldspar to represent the four trenches and are represented at **Table 2.** The chemical analysis for the samples represents that Fe_2O_3 content varies from 2.03% to 2.99% with average of 2.48%, the extremely high amount of iron attributed to the mafic minerals at the original granite of Umm Shaddad. The K_2O content in the analyzed samples range from 4.52% to 5.04% with average of 4.77%, Al_2O_3 from 10.88% to 12.68% with average of 11.7%, Na_2O from 2.54% to 3.33% with average of 3.05%, CaO from 0.55% to 1.82% with average of 0.99% and SiO_2 from72.19% to 75.90% with average of 74.16%

The chemical analysis of Umm Shaddad raw feldspars was compared with the main ingredients of commercial ceramic and glass grade to evaluate the available placer feldspar deposit at Umm Shaddad for use in glass and ceramic industries, **Table 3** and **Table 4;** respectively.

Table 2. The major oxides of seven selected samples (S1-S7) of the Umm Shaddad feldspars and its averages.

Composition	S1	S2	S3	S4	S5	S6	S7	Average
SiO2	72.72	75.35	72.99	75.31	75.90	74.71	72.15	**74.16**
Al2O3	12.37	11.65	12.68	11.63	11.27	10.88	12.08	**11.79**
Fe2O3	2.99	2.35	2.74	2.38	2.60	2.03	2.27	**2.48**
K2O	4.68	4.86	5.04	4.71	4.61	4.52	4.96	**4.77**
Na2O	3.19	3.05	3.33	3.02	2.54	3.07	3.18	**3.05**
MgO	0.36	0.18	0.21	0.17	0.28	0.26	0.35	**0.26**
CaO	0.97	0.55	0.77	0.69	0.55	1.59	1.82	**0.99**
TiO_2	0.23	0.14	0.19	0.15	0.19	0.14	0.17	**0.17**
Total	**97.51**	**98.13**	**97.95**	**98.06**	**98.39**	**97.2**	**96.98**	**97.74**

Table 3. Chemical composition of the main ingredients of commercial ceramic grade feldspar (Loughbrough 1993).

Constituent	Commercial ceramic grade (%)	Average content of samples (%)
SiO_2	75	74.16
Al_2O_3	15	11.19
Fe_2O_3	0.3	2.48
K_2O	3.3	4.77
Na_2O	4.5	3.05

Table 4. Comparison between the chemical composition of the main ingredients of commercial glass grade feldspar given by Harben [18] and the average content of studied samples.

Constituent	Commercial glass grade (%)	Average content of samples (%)
SiO_2	68.90	74.16
Al_2O_3	18.75	11.79
Fe_2O_3	0.07	2.48
K_2O	3.85	4.77
Na_2O	7.15	3.05
CaO	1.85	0.99

4.2. Evaluation of the radiometric effect of the Raw feldspar of Umm Shaddad

Twenty-three samples were selected to represent the four trenches at Umm Shaddad area to evaluate the radiometric effect. The concentrations of natural radioactive elements determined in the collected samples are listed in **Table 5**.

Table 5. The values of K (%), eU (ppm), eTh (ppm) and Ra (ppm) in the collected samples.

Sample no.	eU (ppm)	eTh (ppm)	eRa (ppm)	K (%)
1	8	9	5	5.36
2	1	11	4	5.30
3	10	-	8	3.40
4	11	12	5	4.89
5	9	10	4	4.56
6	8	11	4	4.98
7	11	9	5	5.26
8	10	11	5	5.06
9	11	9	5	5.33
10	10	8	5	4.80
11	10	11	4	5.23
12	10	12	4	4.18
13	7	8	6	4.66
14	7	8	3	4.71
15	7	12	4	4.44
16	9	12	5	4.93
17	12	11	4	4.43
18	11	9	5	4.86
19	11	11	4	4.56
20	11	10	5	4.18
21	10	11	4	4.82
22	8	9	6	4.69
23	12	10	5	4.13

4.3. The Conversion of ground radiometric measurements to specific activity

The value of K expressed in percent and values of eU, eTh, and Ra expressed in ppm were converted to activity concentrations (Bq/Kg) by using the conversion factors given by the International Atomic Energy Agency (1979). **Table 6** show the value of specific activity concentrations of natural radioelements.

The activity conc. of ^{238}U, ^{232}Th, ^{226}Ra and ^{40}K ranged from 86.45 to 148.2 Bq/Kg, 32.48 to 48.7 Bq Kg^{-1}, 33.3 to 88.8 Bq $Kg^{-1}$and 1064.2 to 1677.68 Bq Kg^{-1}, respectively. The United Nations Scientific Committee's report on the consequences of atomic radiation [19] discussed the world average concentration of ^{238}U, ^{232}Th and ^{40}K are 35, 30 and 400 Bq/Kg; respectively. The activity concentration of radionuclides of our study,^{232}Th, ^{238}U, ^{226} Ra and ^{40}K exceeds the global average value.

4.4. Evaluation of radiological hazard effects

4.4.1. Radium equivalent activity, Ra_{eq}

The action of radioactive decay based on the presumption that 370 Bq/kg of ^{226}Ra, 259 Bq/kg of ^{232}Th, and 4810 Bq/ kg of ^{40}K provide the same γ ray dose rate, Ra_{eq} is a weighted sum of the activity of the radionuclides ^{226}Ra, ^{232}Th, and ^{40}K. [20]

$$Ra_{eq} = A_{Ra} + 1.43\ A_{Th} + 0.077\ A_K$$

where A_{Ra}, A_{Th} and A_K are the specific activities of ^{226}Ra, ^{232}Th and ^{40}K in Bq/ kg. Ra_{eq} was estimated for the collected rocks and are given in Table 7. The Ra_{eq} values varied from, 193.2 to 243.98 with average value 225.48Bq/kg for studied samples. The gained results are lower than the accepted global standards (370 Bq/kg).

4.4.2. Gamma activity index, I_γ

The following equation [21] was used to determine I_γ index:

$$I_\gamma = \frac{A_U}{300} + \frac{A_{Th}}{200} + \frac{A_K}{3000}$$

The amounts of 238U, 232Th, and 40K, respectively, are expressed as A_U, A_{Th}, and A_K in Bq/kg unit. This formula is based on the observation that radionuclides contribute to external radiation in proportion to their individual exposure rate constants, i.e., ^{40}K: ^{238}U: ^{232}Th = 1: 10: 15. This method calculates an index of gamma irradiation using the total of three distinct activity quotients, with the denominators selected to reflect the distinct exposure rate and provide a sum of one. According to Tzortzis [21], I_γ values ranged from 0.9 to 1.2, with an average value of 1.04 Bq/kg for the samples under study (Table 7). The average values of the analyzed samples' gamma activity index are below the permissible value (2). The findings also showed that the analyzed rock samples had gamma indices $I_\gamma > 1$ that correspond to dose rates less than 1 mSv/y (EC, 1999), which is thought to be the lowest value of dosage rate in air that is safe for the general population [22, 23].

Table 6. The values of specific activity concentrations of natural radioelements.

Sample no.	U($BqKg^{-1}$)*	Th($BqKg^{-1}$)*	Ra($BqKg^{-1}$)*	K ($BqKg^{-1}$)*
1	1677.68	55.5	36.54	98.8
2	1658.9	44.4	44.66	123.5
3	1064.2	88.8	-	123.5
4	1530.57	55.5	48.72	135.85
5	1427.28	44.4	40.6	111.15
6	1558.74	44.4	44.66	98.8
7	1646.38	55.5	36.54	135.85
8	1583.78	55.5	44.66	123.5
9	1668.29	55.5	36.54	135.85
10	1502.4	55.5	32.48	123.5
11	1636.99	44.4	44.66	123.5
12	1308.34	44.4	48.72	123.5
13	1458.58	66.6	32.48	86.45
14	1474.23	33.3	32.48	86.45
15	1389.72	44.4	48.72	86.45
16	1543.09	55.5	48.72	111.15
17	1386.59	44.4	44.66	148.2
18	1521.18	55.5	36.54	135.85

19	1427.28	44.4	44.66	135.85
20	1308.34	55.5	40.6	135.85
21	1508.66	44.4	44.66	123.5
22	1467.97	66.6	36.54	98.8
23	1292.69	55.5	40.6	148.2

* The activity concentration of a sample containing 1.0 ppm of ^{238}U is equivalent to 12.35 BqKg^{-1}, 1.0 ppm by weight of ^{232}Th is equivalent to 4.06 Bq Kg^{-1}, 1.0 ppm of ^{226}Ra is equivalent to 11.1 Bq Kg^{-1}, and 1% of ^{40}K is equivalent to 313 Bq Kg^{-1}.

4.4.3. Alpha Activity index, I_α

Radon descendants release radioactive alpha particles as they decompose, which adhere to aerosols, dust, and other airborne particles. The alpha particles from radon progeny that are deposited on the cells lining our airways after inhalation can damage DNA and perhaps cause lung cancer. The alpha index (I_α) [23; 24; 25] was used to evaluate the extra alpha radiation brought on by radon inhalation from building materials. The following is its definition:

$$I_\alpha = \frac{A_U}{200} \le 1$$

I_α values varied from 0.4 to 0.74 for the samples that were tested, with an average value of 0.5 Bq/kg (**Table 7**). It is evident that the alpha activity index values below the permitted level. Therefore, it can be claimed that the risk of radon inhalation from structures made of these materials is so low that their usage in building construction should be limited.

4.4.4. Hazard indices (H_{ex} and H_{in})

4.4.4.1. *External hazard index, H_{ex}*

The external risk brought on by gamma radiation emissions is measured using the external hazard index (H_{ex}). With the help of the following equation, it was calculated:

$$H_{ex} = A_U/370 + A_{Th}/259 + A_K/4810 \le 1 \quad [27; 28;29]$$

A_U, A_{Th}, and A_K are the specific activity of ^{238}U, ^{232}Th, and ^{40}K, in Bq/kg, respectively, and H_{ex} is the external hazard index. By assuming that the external hazard index's maximum permissible value i. e. equal to 1 corresponding to Ra_{eq}'s upper bound (370 Bq/kg), the external hazard index can be calculated from the

Ra_{eq} expression. For the radiation danger from construction materials to be insignificant, the value of this index must be lower than unity [30]. The highest value of Ra_{eq} must be less than 370 Bq/kg in order for H_{ex} to have a maximum value that is less than unity. The values of H_{ex} varied from 0.66 to 0.87, with an average value of 0.72 Bq/kg for the samples under study (Table 7). It's acceptable value.

4.4.4.2. *Internal hazard index, H_{in}*

The internal exposure to ^{222}Rn and its radioactive offspring is managed by the internal hazard index (H_{in}). The following equation [24; 26] yields it:

$$H_{in} = A_U/185 + A_{Th}/259 + A_K/4810 \leq 1$$

The conc. of ^{238}U, ^{232}Th, and ^{40}K in Bq/kg are denoted as A_U, A_{Th}, and A_K, respectively. The value of H_{in} will be less than 1 if the maximum uranium concentration in the study samples is half of the typical permitted limit [27]. H_{in} should be less than unity for a material to be used safely in the construction of a home. For the examined rock, values of H_{in} ranged from 0.89 to 1.26, with an average value of 1 Bq/kg (Table 7). It's acceptable value.

Table 7. The values of Radium equivalent activity (Ra_{eq}), Gamma activity level (Iγ), activity index (Iα), hazard indices (Hex and Hin) absorbed dose rate, outdoor, indoor and total external effective dose in (mSv/y) of the study samples.

Sample no.	γ	$Ra_{eq}^{€}$	$_{ex}^{\infty}$	$H_{in}^{¥}$	$I_{\alpha}^{£}$	D^{Ω}	$AEDE^{\beta}$ (msv/y)		
							Outdoor	Indoor	Total
1	1.0712	236.93	0.75	0.4	1.02	1.113	0.945	0.16884	137.675
2	1.187	235.99	0.85	0.61	1.18	0.820	0.699	0.124	101.857
3	-	-	-	0.61	-	-	-	-	-
4	1.206	243.02	0.87	0.67	1.24	1.261	1.070	0.191	156.018
5	1.04	212.35	0.75	0.55	1.05	1.093	0.928	0.165	135.360
6	1.07	228.28	0.76	0.4	1.03	1.111	0.944	0.167	137.610
7	1.18	234.523	0.85	0.67	1.21	1.239	1.052	0.187	153.480
8	1.16	241.31	0.83	0.61	1.16	1.235	1.029	0.183	150.070
9	1.19	236.21	0.855	0.67	1.22	1.247	1.059	0.188	154.400
10	1.07	217.63	0.77	0.61	1.10	1.228	1.043	0.186	152.060
11	1.18	234.31	0.84	0.61	1.18	1.230	1.045	0.186	152.290
12	1.09	214.81	0.79	0.43	1.12	1.139	0.968	0.172	141.040
13	0.9	225.35	0.66	0.43	0.89	0.973	0.826	0.147	120.380
14	0.94	193.2	0.66	0.43	0.89	0.980	0.832	0.148	121.332

15	**0.99**	**221.07**	**0.71**	**0.43**	**0.9**	**1.029**	**0.873**	**0.155**	**127.318**
16	**1.12**	**243.98**	**0.80**	**0.55**	**1.10**	**1.172**	**0.995**	**0.177**	**142.122**
17	**1.17**	**215.03**	**0.86**	**0.74**	**1.26**	**1.238**	**1.051**	**0.187**	**153.263**
18	**1.14**	**224.88**	**0.82**	**0.67**	**1.19**	**1.198**	**1.017**	**0.181**	**148.266**
19	**1.15**	**218.16**	**0.83**	**0.67**	**1.2**	**1.205**	**1.023**	**0.182**	**149.130**
20	**1.09**	**214.300**	**0.79**	**0.67**	**1.16**	**1.1462**	**0.973**	**0.173**	**141.879**
21	**1.13**	**224.34**	**0.81**	**0.61**	**1.15**	**1.187**	**1.008**	**0.179**	**146.942**
22	**1.001**	**231.88**	**0.71**	**0.49**	**0.9**	**1.037**	**0.880**	**0.157**	**128.930**
23	**1.12**	**213.09**	**0.82**	**0.741**	**1.2**	**1.186**	**1.007**	**0.179**	**146.895**
Average	**1.04**	**225.48**	**0.72**	**0.5**	**1.1**	**1.137**	**1.008**	**0.169**	**140.853**

[€]The radium equivalent activity Ra_{eq} is a weighted sum of activities of the ^{226}Ra, ^{232}Th and ^{40}K radionuclides based on the assumption that 370 Bq/ kg of ^{226}Ra, 259 Bq/ kg of ^{32}Th and 4810 Bq/ kg of ^{40}K produce the same gamma ray dose rate [19]

$$Ra_{eq} = A_{Ra} + 1.43\ A_{Th} + 0.077\ A_K$$

The gamma activity concentration index I_γ was calculated from the following equation [21]:

$$I_\gamma = \frac{A_U}{300} + \frac{A_{Th}}{200} + \frac{A_K}{3000}$$

[£] Alpha index (I_α), defined as follows [24; 25;26]: $I_\alpha = \frac{A_U}{200} \leq 1$

[∞] External hazard index (H_{ex}) calculated by the equation from [27,28 and 29]: $H_{ex} = A_U/370 + A_{Th}/259 + A_K/4810 \leq 1$

[¥]The internal hazard index (H_{in}) calculated by the equation from [27 ,28 and 29]: $H_{in} = A_U/185 + A_{Th}/259 + A_K/4810 \leq 1$

[Ω]The absorbed dose rate (D) was calculated using the conversion factors specified by **[19]** as follow:

D (nGy/h) = 0.429 × U + 0.666 × Th + 0.042 × K ……. (Eq. 1)

Where U, Th and K are the specific activity concentration of ^{238}U, ^{232}Th and ^{40}K in (Bq/Kg); respectively.

[β]The annual effective dose equivalent (AEDE) in indoor and outdoor air was determined according to **[23]** as follow:

AEDE (outdoors) = *D* (nGy/h) × 8760 (h/y) × 0.2 × 0.7 (Sv/Gy^{-1}) × 10^{-6} (mSv/y) …. (Eq. 2)

Where, D: Absorbed Dose (nG/yh); 8760 (h/y): Time of hours per one year; 0.2: Occupancy factor for outdoor (5/24) and 0.7: Conversion Coefficient for adult from absorbed dose to effective dose (Sv/Gy^{-1}).

AEDE (indoors) = *D* (nGy/h) × 1.4 × 8760 (h/y) × 0.8 × 0.7 (Sv/Gy^{-1}) × 10^{-6} (mSv/y) …... (Eq. 3)

Where, D: Absorbed Dose (nG/yh); 1.4: Population weighted value, because the indoor exposures are 40% greater than the outdoor exposures; 8760 (h/y): Time of hours per one year; 0.8: Occupancy factor for indoor (5/24) and 0.7: Conversion Coefficient for adult from absorbed dose to effective dose (Sv/Gy^{-1}).

4.4.5. Absorbed Dose

According to [18], the absorbed dose rate was computed (Eq. 1) and its values are reported in Table 7. The absorbed dose rate is defined as the quantity of energy in a unit mass in human tissues or organs. having a mean value of 140.853 nG/h, the computed values of the absorbed dosage varied from 101.8 to 156.01 nG/h. It exceeds the global average of 60 nG/h [23].

4.4.6. Annual effective dose equivalent (AEDE)

Gamma radiation from radionuclides in the ^{238}U and ^{232}Th series as well as from the presence of ^{40}K in collected samples are the main causes of external irradiation of the human body. Additionally, if earth materials are utilized during building, indoor gamma exposure which is primarily influenced by these elements—is naturally higher than outdoor exposure. The importance of indoor exposure increases when the length of tenancy is considered [23].

The conversion coefficient from absorbed dosage in air to effective dosage and the outdoor and indoor occupancy factors are utilized to estimate the annual effective doses, according to Senthilkumar and Narayanaswamy [31]. The study of [23] states that the conversion coefficient between the absorbed dosage in the air and the effective dose received by humans is 0.7 Sv/Gy, and the occupancy factor for outdoor and indoor is, respectively, 0.2 and 0.8, meaning that, in terms of time spent indoors and outside. According to UNSCEAR [23], the annual effective dose equivalent (AEDE) in both outdoor and indoor air was calculated. Table 7 lists the computed AEDE indoor (Eq. 2) and outdoor (Eq. 3) values.

The indoor and outdoor AEDE values range from 0.69 to 1.07 mSv/y and from 0.123 to 0.191 mSv/y, respectively (outdoor). The annual effective dose as a result is 0.48 mSv/y on average across the globe [22].

4.4.7. Total annual effective dose

The sum of AEDE, indoor (mSv/y) and AEDE, out (mSv/y) yields the total annual effective dose equivalent, Total (mSv/y). Total AEDE in the study samples varied from 0.82 to 1.261, with an average of 1.137. The annual effective dosage from external terrestrial radiation for the entire world's population is 0.5 mSv [23].

5. Conclusions

When compared to the commercial average for these economic industries, with the investigated feldspar placer deposit of the area under consideration. The chemical investigation revealed that Fe_2O_3 had an average concentration of 2.48%, which is extremely high. The average K_2O content in the samples was 4.77%, the average Al_2O_3 content was 11.79% less than the commercial average for the ceramic and glass industries, the average Na_2O content ranged from 2.54% to 3.33% less than the commercial average for the ceramic and glass industries, and the average SiO2 content was 74.16% less than the commercial average for the ceramic industries but higher than the commercial average for the glass industries. For the samples under study, Ra_{eq} ranged from 193.2 to 243.98 with an average value of 225.48Bq/kg. The measured levels are below the permissible global threshold (370 Bq/kg). I_γ values for the study samples varied from 0.9 to 1.2, with an average value of 1.04 Bq/kg. The gamma activity index average values of the examined samples fall below the allowable value (2). I_α values for the samples under investigation ranged from 0.4 to 0.74 Bq/kg on average. Values for the alpha activity index are below the allowable range. H_{ex} values for the samples that were evaluated varied from 0.66 to 0.87, with an average value of 0.72 Bq/kg, which is an acceptable value. The analyzed rock's H_{in} values ranged from 0.89 to 1.26, with an average value that is acceptable being 1 Bq/kg. Wherever, the total annual effective dose equivalent total AEDE in the studied samples ranged from 0.82 to 1.261 with an average of 1.137, which exceeding the global effective dose from external terrestrial radiation for the entire population, which is 0.5 mSv/year. where the examined feldspars' effective dose exceeds the global effective dose. In conclusion, although the feldspar placers of Umm Shaddad area have suitable content of oxides after minor treatment while, the high values of total Annual effective dose equivalent (AEDE) diminished its use for either ceramic or glass industries.

6. Acknowledgements

Our research received no grants from any funding agencies in public, non-profit or commercial sectors. The kind help of Prof. Adel El-Afandy, Nuclear Material Authority, Cairo, Egypt and Mahmoud El Tawabty, Miss Asmaa Nazir, Faculty of Science, Damietta University is greatly appreciated.

7. REFERENCES

[1] M. Dondi, "Feldspars and other fluxes for ceramic tiles: sources, processing, composition and technological behavior", CRAM raw materials profile, European innovation partnership on raw materials, 1st edition, p260, 2018, doi: 10.1016/b978-044450945-1/50092-0.

[2] Roskill Information Services Ltd., "The economics of feldspar", 11th ed, Roskill information services Ltd., London, United Kingdom, p320, 2008, doi: 10.1093/ww/9780199540884.013.u175191.

[3] M. Garside, 2022: "Feldspar mine production in Egypt 2010-2020", Statista.com, 2022.

[4] M. Izquierdo Pazo, M. L. Andrade Couce, M. Bao Iglesias, and P. Arcet Miramontes, "Obtention of feldspar raw material for porcelain and ceramic industries from biotite-porphyritic granite (Porrino Granite)," Silic Ind vol. 62 no. 5/6, 97-104, 1997, doi: 10.2991/gmee-15.2015.18.

[5] E. Rau, "Feldspar," In: N. L. Weiss (Ed.). SME mineral processing handbook. New York: Society of Mining Engineers of the American Institute of Mining, Metallurgical and Petroleum Engineers, 1985, doi: 10.1002/jctb.5000500212.

[6] H. F. El-Maghraby, M. M. El-Omla, F. Bondioli, and S. M. Naga, "Granite as flux in stoneware tile manufacturing," Journal of the European Ceramic Society, vol. 31 no. 12, 2057-2063, 2011, Doi: 10.1016/j.jeurceramsoc.2011.05.023.

[7] S. M. Naga, F. Bondioli, M. M. S. Wahsh, and M. El-Omla, "Utilization of granodiorite in the production of porcelain stoneware tiles. Ceramics International, vol. 38 no. 8, 6267-6272, 2012, doi: 10.1016/j.ceramint.2012.04.081.

[8] H.F. El-Maghraby, Mohamed M. El-Omla, F. Bondioli, S.M. Naga, "Granite as flux in stoneware tile manufacturing," Journal of the European Ceramic Society vol. 31 no. 12 pp 2057 - 2063, 2011, doi: 10.1016/j.jeurceramsoc.2011.05.023.

[9] D. M. Ibrahim, E. H. Sallam, and S. M. Naga, "Effect of the degree of crystallinity of flux on tile bodies," Interbrick, vol. 11, no. 4, 7-10, 1990, doi: 10.1016/0272-8842(84)90008-7.

[10] S. E. Ahmed, S. A. El Rahim, D. A. Aziz, and N. A. El Ghaffar, "Utilization of granite in the Umm Had area. Central Eastern Desert. Egypt. As fluxing Material in the Preparation of Ceramic Recipes," Interceram, vol. 6, 438-443, 2013, doi: 10.1016/j.ceramint.2020.07.334.

[11] H. M. Abdalla, S. Ishihara, H. Matsueda, and A. A. Monem, "On the albite-enriched granitoids at Um Ara area. South Eastern Desert. Egypt. 1. Geochemical ore potentiality and fluid inclusion studies," Journal of Geochemical Exploration, vol. 57, no. 1-3, 127-138, 1996, doi: 10.1016/s0375-6742(96)00029-5.

[12] H. Helba, R. B. Trumbll, G. Morteani, S. O. Khalil, and A. Arslan, "Geochemical and petrographic studies of Ta mineralization in the Nuweibi albite granite complex. Eastern Desert. Egypt," Mineralim Deposita, vol. 32, no. 2, 164-179, 1997, doi: 10.1007/s001260050082.

[13] H. Abdalla, "Mineralogical and Geochemical characterization of Beryl-bearing Granitoids. Eastern Desert. Egypt: Metallogenic and Exploration Constrains," Resource Geology, vol. 59, no. 2, 121-139, 2009, doi: 10.1111/j.1751-3928.2009.00085.x.

[14] Conoco Coral, "The Geological map of Egypt (Gabal Hamata)," Institute fur Angewandte Geodasie, Berline Techniche Fachhochashule Berline, 1987, Doi:10.4043/5585-ms.

[15] M. M. El-Sayed, M. A. Hassanen, and M. A. Obeid, "Geochemistry and petrogenesis of Late Precambrian tonalite - granodiorite - syenogranite series at Umm Shaddad district (Egypt)," Journal of Mineralogy and Geochemistry, vol. 175, no. 1, 29-51, 1999, doi: 10.1127/njma/175/1999/29.

[16] A. H. Sabet, "Geology and mineralogy of Gabal El-Sibai area, Red Sea hills, Egypt," PhD Thesis, Leiden state University, the Netherlands, 1961, doi: 10.21608/djs.2005.158266.

[17] R. Loughbrough, "Portugal's minerals," Industrial minerals, vol. 308, no. 1, 51-52, 1993, doi: 1080/00357529.1976.11762097.

[18] P. W. Harben, "The industrial minerals handbook: A guide to markets, specifications and prices," Metal Bulletin, PLC, industrial minerals division, 2nd ed. London, vol. 20 no.4 pp: 62-65, 1995, doi: 10.1016/0301-4207(94)90012-4.

[19] UNSCEAR, "Sources and biological effects of ionizing radiation," Report to the General Assembly of the United Nations with Scientific Annexes, United Nations sales publication E.82. IX.8, New York, 1988, doi: 10.18356/55345362-en.

[20] G. A. Ravisankar, R. Sarada, S. Vidyashankar, K. S. Venu Gopal, and A. Kumudha, "Cultivation of micro-algea for lipids and hydrocarbons, and utilization of spent biomass for livestock feed and for bio-active constituents," In: Makkar, H.P.S, Biofuel co-products as livestock feed-opportunities and challenges, FAO, pp. 423-446, 2012, doi: 10.18356/1880e75c-en.

[21] M. Tzortzis, "Gamma radiation measurements and dose rates in commercially-used natural tiling rocks (granites)," Journal of Environmental Radioactivity, vol. 70, no. 3, 223-35, 2003, doi: 10.1016/s0265-931x (03)00106-1.

[22] UNSCEAR, "Sources and effects of ionizing radiation," Report to the General Assembly of the United Nations with Scientific Annexes, United Nations sales publication E.00.IX.3, New York, 1993, doi: 10.18356/a71e0e29-en.

[23] UNSCEAR, "Sources and effects of ionizing radiation," Report to the General Assembly of the United Nations with Scientific Annexes, United Nations sales publication E.00.IX.3, New York, 2000, doi: 10.18356/28d343af-en.

[24] E. Bavarnegin, M. Moghaddam, B. Asad, and N. Fathabadi, "Analytical study of radionuclide concentration and radon exhalation rate in market available building materials of Ramsar," Journal of Theoretical and Applied Physics, vol. 6, no. 1, 5, 2013, doi: 10.1186/2251-7235-6-5.

[25] S. Righi, and L. Bruzzi, "Natural radioactivity and radon exhalation in building materials used in Italian dwellings," Journal of Environmental Radioactivity vol. 88, no. 2, 158-170, 2006, doi: 10.1016/j.jenvrad.2006.01.009.

[26] M. Zubair, S. Hassan, K. Rizwan, N. Rasool, M. Riaz, M. Ziaul-Haj, and V. D. Feo, Antioxidant potential and oil composition of Callistemon viminalis leaves," The Scientific World Journal, 2013: article ID 489071, 2013, doi: 10.1155/2013/489071.

[27] J. Beretka, and P. J. Mathew, "Natural radioactivity of Australian building materials, industrial wastes and by-products," Health Physics, vol. 48, no. 1, 87-95, 1985, doi: 10.1097/00004032-198501000-00007.

[28] Y. Orgun, N. Altinsoy, S. Y. Sahin, Y. Gungor, A. H. Gultekin, G. Karahan, and Z. Karacik, "Natural and anthropogenic radionuclides in rocks and beach sands from Ezine region (Canakkale), Western Anatolia, Turkey," Applied Radiation and Isotopes, vol. 65, no. 6, 739-747, 2013, doi: 10.1016/j.apradiso.2006.06.011.

[29] S. Fares, J. K. Park, D. R. Gentner, R. Weber, E. Ormeno, J. Karlik, and A. H. Goldstein, "Seasonal cycles of biogenic volatile organic compound fluxes and concentrations in a California citrus orchard," Atmospheric Chemistry and Physics, vol. 12, no. 20, 9865-9880, 2012, doi: 10.5194/acp-12-9865-2012.

[30] P. Hayumbu, M. B. Zaman, N. C. H. Lubaba, S. S. Munsanje, and D. Nuleya, Natural radioactivity in Zamibia building materials collected from Lusaka. J. Radio analytical and Nuclear Chemistry, vol. 199, no. 3, 229-238, 1995, doi: 10.1007/bf02162371.

[31] R.D. Senthilkumar, and R. Narayanaswamy, "Assessment of radiological hazards in the industrial effluent disposed soil with statistical analyses," J. Rad. Res. App Sci. vol. 9, no. 1, 449-456, 2016, doi: 10.1016/j.jrras.2016.07.002.